BMC Cancer

RESEARCH

Open Access

HIST3H2A promotes the progression of prostate cancer through inhibiting cell necroptosis

Lihong Yang[1], Yong Ruan[2] and Houqiang Xu[1,2*]

Abstract

In recent years, there has been an increase in the incidence and mortality rates of prostate cancer (PCa). However, the specific molecular mechanisms underlying its occurrence and development remain unclear, necessitating the identification of new therapeutic targets. Through bioinformatics analysis, we discovered a previously unstudied differential gene called HIST3H2A in prostate cancer. Our study revealed that HIST3H2A is highly expressed in PCa tissues, as confirmed by analysis of both the GEO and UALCAN databases. Further analysis using the KEGG database demonstrated that HIST3H2A regulates the pathway of programmed necroptosis in cells. Additionally, we observed significant up-regulation of HIST3H2A in PCa tissues and cell lines. HIST3H2A was found to regulate cell proliferation, migration, invasion, and the epithelial-mesenchymal transition (EMT) process in tumors. Notably, HIST3H2A's role in regulating programmed necroptosis in prostate cancer cells differs from its role in apoptosis. In vitro and in vivo experiments collectively support the key role of HIST3H2A in promoting the development of prostate cancer, highlighting its potential as a therapeutic target for patients with PCa.

Keywords Prostate cancer, HIST3H2A, Progression, Necroptosis

Introduction

Prostate cancer (PCa) is the second most common cancer in men worldwide, with increasing incidence and mortality rates [1–3]. Despite advancements in diagnosis and treatment, the molecular mechanisms underlying prostate cancer development remain incompletely understood. Therefore, there is a critical need to identify new potential biomarkers and uncover unknown pathogenic factors. Mammalian cells undergo different forms of cell death, such as apoptosis, necroptosis, and pyroptosis, under various stress conditions [4–7]. Dysregulation of cell death processes can contribute to various human diseases, including cancer, neurodegeneration, and infectious diseases [8–11]. In the context of cell necroptosis, the protein kinase Receptor-interacting protein 3 (RIP3) plays a crucial role [12–14]. RIP3 is a serine/threonine kinase that consists of a homologous N-terminal kinase domain and a unique C-terminal domain [15–17]. Upon activation, RIP3 recruits and phosphorylates the lineage kinase domain-like protein (MLKL), leading to its oligomerization and localization to the plasma membrane. Ultimately, this results in cell membrane rupture and cell death [15, 18–20].

Nucleosomes, composed of histones H2A, H2B, H3, and H4, are the fundamental units of chromatin fibers in eukaryotic cells [21–23]. Each nucleosome consists of two units of H3 and H4, forming a tetramer surrounded

*Correspondence:
Houqiang Xu
gzdxxhq@163.com
[1]Key Laboratory of Animal Genetics, Breeding and Reproduction in the Plateau Mountainous Region, Ministry of Education, College of Life Sciences, Guizhou University, Guiyang 550025, China
[2]College of Animal Science, Guizhou University, Guiyang 550025, China

by two dimers of H2A-H2B [24–26]. Variants of H2A, H2B, and H3 have been identified in eukaryotes, and certain variants of H2A have been linked to cancer [27, 28]. For instance, H2A.z is believed to have pro-tumor effects [29–31], while macroH2A and H2A.x are considered tumor inhibitors [32]. Deletion or mutation of the H2A.X gene can lead to severe DNA damage and has been associated with the development of various cancers, including breast cancer, head and neck squamous cell carcinoma, neuroblastoma, and hematopoietic malignancies [33–39]. Although the involvement of H2A family protein variants, such as H2A.Z-1 and H2A.Z-2, in prostate cancer has been established, the HIST3H2A underlying mechanism remains unclear.

In this study, we investigated the significance of HIST3H2A expression in prostate cancer. Our findings demonstrate that HIST3H2A expression may influence the occurrence and progression of prostate cancer. Specifically, HIST3H2A is significantly up-regulated in both human prostate cancer tissues and prostate cancer cells. Overexpression of HIST3H2A promotes cell proliferation, migration, and invasion, whereas interference with HIST3H2A inhibits the proliferation of prostate cancer cells and significantly reduces their migration and invasion capabilities. Notably, this process is mediated through programmed necroptosis rather than apoptosis. Collectively, our study suggests that HIST3H2A plays a crucial role in inducing cell death and could serve as a potential therapeutic target for prostate cancer.

Methods and materials

Data sources

The PCa mRNA datasets GSE 69,223, GSE 32,571, GSE 6919, and GSE 46,602 were obtained from the GEO database (https://www.ncbi.nlm.nih.gov/geo/). Subsequently, the UALCAN database (https://ualcan.path.uab.edu) was utilized to analyze the expression differences between cancerous and non-cancerous tissues. Additionally, the KEGG database was employed to identify the pathways regulated by HIST3H2A.

Tissue and cell lines

Tissue chips were purchased from Servicebio Biotechnology Co., LTD (Wuhan, China). Human prostate cancer cell lines (PC3, 22RV1) and human normal prostate epithelial RWPE-1 cells were obtained from Zhongqiao Xinzhou Biotechnology (Shanghai, China).

Table 1 The primers used for real-time PCR

Primer	Sequence	Product size (bp)
GAPDH-F	TGCAACCGGGAAGGAAATGA	148
GAPDH-R	GCATCACCCGGAGGAGAAAT	
HIST3H2A-F	GTCTCGCTTTTCGGTTGCC	74
HIST3H2A-R	CTTGCCACCCTGCTTACCA	

Cell culture and transfection

PC3 cells were cultured in DMEM-F12 medium (Gibco, NY, USA) supplemented with 10% fetal bovine serum (VivaCell, China) and 1% streptomycin-penicillin (Gibco, NY, USA). 22RV1 cells were cultured in RPMI-1640 medium (Gibco, NY, USA) supplemented with 10% fetal bovine serum (VivaCell, China) and 1% streptomycin-penicillin (Gibco, NY, USA). RWPE-1 cells were sustained in a specialized medium for RWPE-1 cells (ZQ-1303, ZQXZ Bio, Shanghai, China). All cells were cultured at 37 °C in a CO_2 incubator with 5% CO_2. pcDNA3.1-HIST3H2A (oe-HIST3H2A) and LV-HIST3H2A vectors were obtained from Tsingke (Chongqing, China), and corresponding negative controls (NC) were also obtained. Cells were transfected with the specific vector using FuGENE HD (Promega, Madison, WI, USA) reagents following the instructions for use, and then used for further research.

Real-time quantitative PCR (qRTPCR)

Total RNA was extracted from PC3, 22RV1, and RWPE-1 cells using the Trizol method (Invitrogen, Carlsbad, CA, USA) following the manufacturer's instructions. RNA quality was assessed using ultraviolet spectrophotometry (Invitrogen, Carlsbad, CA, USA). For RNA reverse transcription, the RevertAid First Strand cDNA Synthesis kit from Invitrogen was employed. The qRT-PCR experiment was conducted using the CFX-96 Real-Time PCR system and Bio-Rad Laboratories SYBR Green Mix, with specific thermal cycle conditions set. The initial predenaturation step was performed at 95 °C for approximately 3 min, followed by 39 cycles of 30 s at 95 °C, 5 s at 57 °C, and 30 s at 72 °C. Three independent replicates were collected in this study, and mRNA expression levels were measured using GAPDH as an internal control. Data were analyzed using the $2^{-\Delta\Delta Cq}$ method [40]. The primers used for real-time PCR are listed in Table 1.

Western blot

Proteins were extracted from cells using the radioimmunoprecipitation assay (RIPA) lysis buffer (Solarbio, China). The concentrations were determined using the bicinchoninic acid (BCA) protein assay (Solarbio, China). The extracted proteins were then electrophoresed on SDS-polyacrylamide gels and transferred to PVDF membranes (Millipore, Carrigtwohill, Ireland). After sealing with skim milk, the membranes were incubated overnight at 4 °C with the primary antibody. Subsequently, the membranes were washed and incubated with the secondary antibody at room temperature for 2 h. The antibodies used in this study were as follows: anti-HIST3H2A (1:1000 dilution; Proteintech, USA), anti-Bax (1:5000 dilution; Proteintech, USA), anti-MMP-9 (1:1000 dilution; Proteintech, USA), anti-MMP-2 (1:1000 dilution;

Proteintech, USA), anti-E-cadherin (1:5000 dilution; Proteintech, USA), anti-N-cadherin (1:1000 dilution; Proteintech, USA), anti-PCNA (1:3000 dilution; Proteintech, USA), anti-Vimentin (1:5000 dilution; Proteintech, USA), anti-Caspase 9 (1:1000 dilution; Proteintech, USA), anti-CDK6 (1:5000 dilution; Proteintech, USA), anti-Cyclin D1 (1:5000 dilution; Proteintech, USA), anti-Bcl-2 (1:2000 dilution; Proteintech, USA), anti-Cyclin E1 (1:1000 dilution; Proteintech, USA), anti-CDK2 (1:1000 dilution; Proteintech, USA), GAPDH (1:1000 dilution; Proteintech, USA), and goat-anti-rabbit, goat-anti-mouse secondary antibody (1:10000 dilution; Proteintech, USA), anti-RIP3 (1:2000 dilution; Proteintech, USA), anti-p-RIP3 (1:2000 dilution; Affinity, USA), anti-MLKL (1:5000 dilution; Proteintech, USA), and anti-p-MLKL (1:1000 dilution; Affinity, USA). The results were quantified and the images were processed using Image J software.

Immunohistochemistry

Immunohistochemistry (IHC) was employed to section mouse tumor tissue as described in a previous study [41]. The primary antibody used for IHC was the same as the one used for the western blot analysis. Tissue sections were incubated overnight at 4 °C with the primary antibody, followed by incubation with the secondary antibody. The DAB complex was utilized as a chromogen to visualize the target antigen. Nuclei were counterstained with hematoxylin.

EdU assay

The impact of HIST3H2A on the proliferation of PC3 and 22RV1 cells was assessed using the EdU (APExBIO, USA) methods. In the EdU detection, the cells were transfected with either vector or shRNA for 48 h before being seeded in 24-well plates at a density of 2×10^5 cells per well. The cells were then incubated with 20 mM EdU for 2 h. After fixing with 3.7% formaldehyde for 15 min and permeabilizing with 0.25% Triton X-100 for 15 min at room temperature, the cells were washed 3 times with PBS and incubated with Click buffer for 30 min at room temperature. The uptake rate of EdU was determined by calculating the ratio of the total number of EdU-positive cells (red) to the total number of blue cells after Hoechst 33,258 staining.

Cell migration and invasion assays

After transfection, 1.5×10^5 PC3 and 22RV1 cells were cultured in 180 μL of complete culture medium and inoculated into the upper chambers of a transwell (pore size 8 mm, Costar). Matrigel was added to the upper chambers for invasion experiments, but not for migration experiments. A chemo-attractant consisting of 600 μL complete growth medium and 15% fetal bovine serum was added to the bottom well of each chamber. The cells were then incubated for 24 h at 37 °C and 5% CO2 for migration and invasion assays. After incubation, the cells from the upper chamber were scraped off with a cotton swab. The invasive cells on the other side were fixed with 3.7% paraformaldehyde, stained with Giemsa, and photographed using a microscope (Nikon, Japan).

Xenograft tumor model

The animal experiment was conducted in accordance with the guidelines set by the Committee for Animal Care and Use of Guizhou University according to the Basel Declaration. To establish the mouse tumor model, 5-week-old BALB/c nude mice (Tengxin Biotechnology, Chongqing, China) were randomly divided into two groups ($n=7$ per group): one group received cells with Lentiviral shRNA control vector (HIST3H2A-NC) and the other group received cells with Lentiviral shRNA vector (HIST3H2A-shRNA). The cells were injected subcutaneously into the nude mice at a concentration of 4×10^6 cells in 0.2 mL of PBS per mouse. At the end of the 4-week period, the mice were euthanized using an overdose of pentobarbital (250 mg/kg intraperitoneal injection). Once it was confirmed that the mice had passed away as a result of respiratory and cardiac arrest, the tumor tissues were collected and subjected to immunohistochemistry (IHC) staining.

Statistical analysis

The statistical data was obtained from triple repetitions using GraphPad Prism 9 (GraphPad, La Jolla, CA, USA) and is presented as mean ± SD. To analyze the statistical significance differences between the two datasets, a two-tailed Student's t-test was performed. A p-value of less than 0.05 was considered statistically significant.

Results

Screening and expression analysis of HIST3H2A

To identify potential molecular targets for prostate cancer, we conducted bioinformatics analyses using four databases: GSE 69,223, GSE 32,571, GSE 6919, and GSE 46,602. Our analysis revealed that there were 13,312 genes common to all four databases (Fig. 1A). Among these genes, we found that HIST3H2A was highly expressed in prostate cancer and had not been previously studied in this context (Fig. 1B). Further analysis using the UALCAN database confirmed that HIST3H2A expression in prostate cancer was significantly higher than in adjacent prostate cancer tissues (Fig. 1C). To validate these findings, we performed additional experiments using tissue microarray IHC (Tumor, 59 point and Normal, 27 point), qRT-PCR, and western blot. Consistently, our results showed that HIST3H2A expression was significantly higher in prostate cancer tissues compared to adjacent prostate cancer tissues (Fig. 1D). Moreover, both

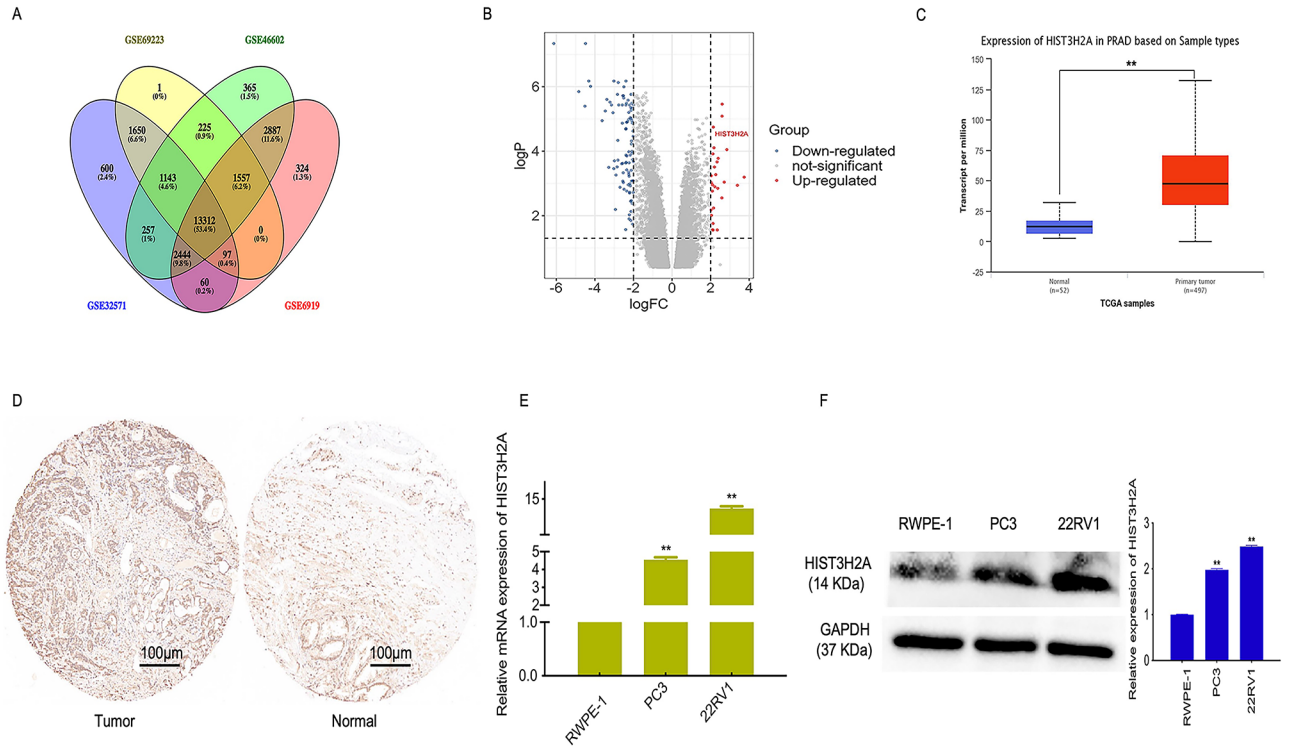

Fig. 1 Screening and expression analysis of HIST3H2A. **A** Differential gene screening. **B** Fold change of differential gene. **C** Analysis of expression difference between cancer and paracancer in UALCAN database. **D** HIST3H2A expression between PCa tumor tissue and adjacent non-tumor tissue by tissue chip IHC. **E** HIST3H2A expression level detected in prostate cancer cell lines (PC3 and 22RV1) and normal prostate RWPE-1 cells by qRT-PCR. **F** HIST3H2A expression level detected in prostate cancer cell lines (PC3 and 22RV1) and normal prostate RWPE-1 cells by western blot. Scale bars 100 μm. $*p < 0.05$, $**p < 0.01$ by Student's t-test. Error bars indicate SD

qRT-PCR and western blot analyses demonstrated that HIST3H2A expression was significantly higher in PC3 and 22RV1 cells, two prostate cancer cell lines, compared to normal prostate RWPE-1 cells (Fig. 1E and F).

HIST3H2A regulates cells proliferation

To investigate the role of HIST3H2A in cell proliferation, we conducted several assays including western blot, 5-ethynyl-20-deoxyuridine (EdU) incorporation. The western blot analysis revealed that HIST3H2A was overexpressed in PC3 cells (Fig. 2A), while successful interference with HIST3H2A was achieved in 22RV1 cells (Fig. 2B). Overexpression of HIST3H2A in PC3 cells resulted in increased expression of proliferation-related proteins such as PCNA, CDK2, CDK6, cyclinD1, cyclinE1, and decreased expression P21 (Fig. 2C and E). Conversely, interference with HIST3H2A in 22RV1 cells led to the opposite result (Fig. 2D and F). Similar findings were observed through EdU incorporation assay (Fig. 2G).

HIST3H2A regulates EMT process

When tumor cells invade and metastasize, they tend to lose polarity and epithelial characteristics, such as changes in the expression of proteins like E-cadherin, N-cadherin, and Vimentin, and acquire mesenchymal phenotypes similar to the enhancement of MMP expression. This phenomenon is known as the epithelial-to-mesenchymal transition (EMT). In this study, western blot and transwell tests were conducted to detect cell invasion, migration, and metastasis. The western blot results showed that overexpression of HIST3H2A in PC3 cells significantly increased the expression levels of invasion-related genes MMP-2 and MMP-9, decreased the expression levels of E-cadherin, and increased the expressions of N-cadherin and Vimentin (Fig. 3A and E). On the other hand, interference of HIST3H2A in 22RV1 cells led to a significant decrease in the expression levels of invasion-related genes MMP-2 and MMP-9, an increase in the expression levels of E-cadherin, and a decrease in the expression levels of N-cadherin and Vimentin (Fig. 3B and F). The Transwell assay also demonstrated that overexpression of HIST3H2A promoted the invasion and migration of PC3 cells (Fig. 3C), while interference with HIST3H2A inhibited the invasion and migration of 22RV1 cells (Fig. 3D).

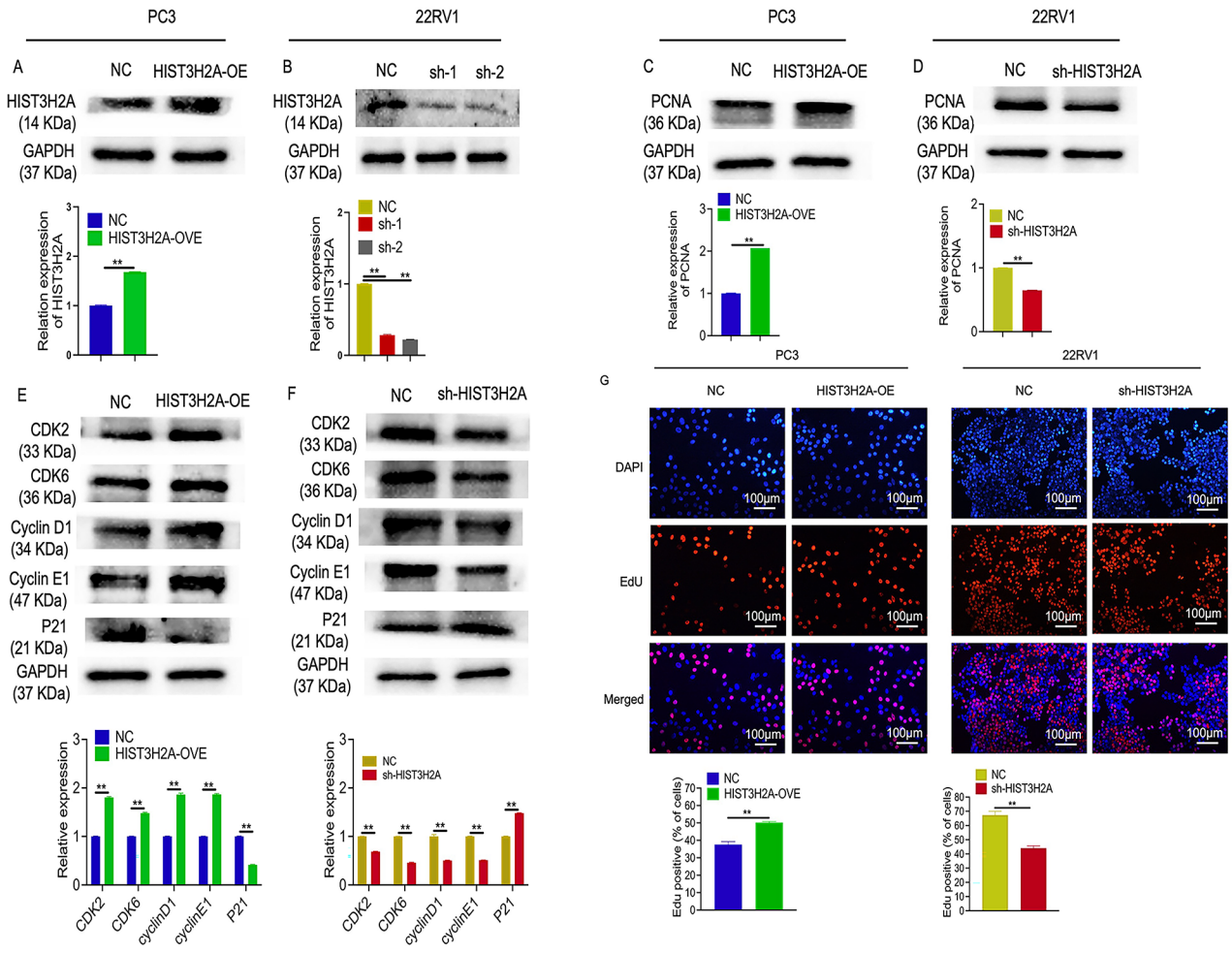

Fig. 2 HIST3H2A regulates Cells proliferation. **A** HIST3H2A overexpression efficiency detection by western blot. **B** HIST3H2A interference efficiency detection by western blot. **C** The effect of HIST3H2A overexpression on the proliferation-related gene by western blot. **D** The effect of HIST3H2A interference on the proliferation-related gene by western blot. **E** The effect of HIST3H2A overexpression on the cycle-related gene by western blot. **F** The effect of HIST3H2A interference on the cycle-related gene by western blot. **G** The effect of HIST3H2A overexpression or knockdown on the proliferation of PC3 and 22RV1 cells were assessed by EdU. Scale bars 100 μm. *$p < 0.05$, **$p < 0.01$ by Student's t-test

HIST3H2A regulates cells proliferation through necroptosis but not through apoptosis

To investigate the role of HIST3H2A in regulating the proliferation of prostate cancer cells, we examined the expression of apoptosis-related proteins Caspase 9, Bax, and Bcl-2. Western blot analysis revealed that overexpression or interference of HIST3H2A had no significant effect on the levels of these proteins in PC3 and 22RV1 cells (Fig. 4A and B). Additionally, the results of JC-1 staining showed that HIST3H2A interference or overexpression did not impact cell apoptosis (Fig. 4C and D). These findings suggest that HIST3H2A does not influence prostate cancer cell proliferation through apoptosis regulation. However, according to the KEGG database, HIST3H2A may be involved in the regulation of necroptosis (Fig. 4G). To further explore this, we performed western blot analysis to assess necroptosis-related proteins. We observed that the expression of RIP3, p-RIP3, MLKL, and p-MLKL decreased upon HIST3H2A overexpression in PC3 cells (Fig. 4E), while it increased after HIST3H2A interference in 22RV1 cells (Fig. 4A and F). Overall, our results suggest that HIST3H2A regulates cell proliferation through necroptosis rather than apoptosis.

HIST3H2A regulates tumor growth in vivo

To further investigate the role of HIST3H2A in regulating prostate cancer progression in vivo, we conducted a xenograft tumor model in nude mice. Our results from the xenografted mice model demonstrated that the LV-HIST3H2A groups exhibited a significant decrease in tumor growth compared to the control xenografts (Fig. 5A). These findings indicate that interference with HIST3H2A inhibited the formation and growth of

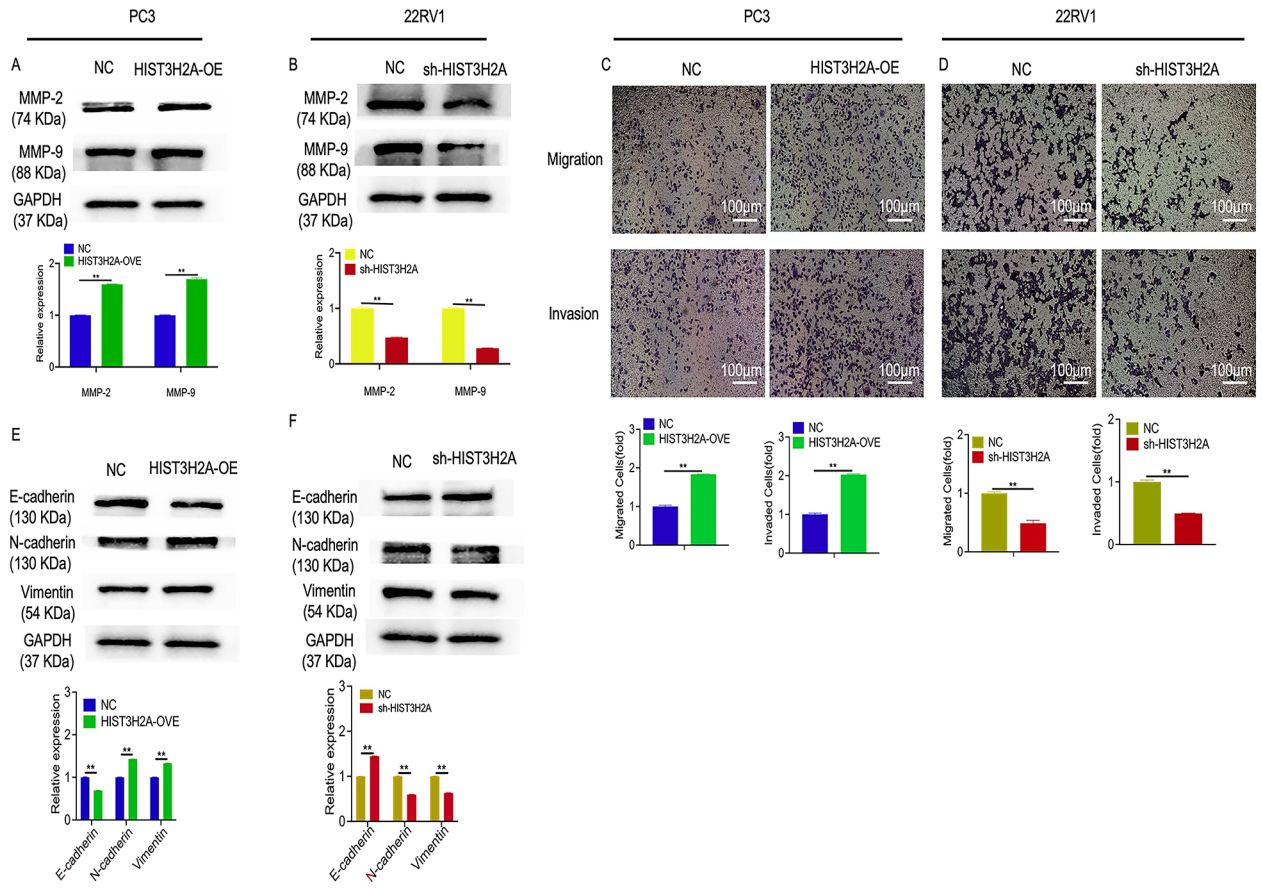

Fig. 3 HIST3H2A regulates EMT process. **A** The effect of HIST3H2A overexpression on the tumor invasion and metastasis genes by western blot. **B** The effect of HIST3H2A interference on the tumor invasion and metastasis genes by western blot. **C** The effect of HIST3H2A overexpression on the migration and invasion by transwell assay. **D** The effect of HIST3H2A interference on the migration and invasion by transwell assay. **E** The effect of HIST3H2A overexpression on the EMT-related gene by western blot. **F** The effect of HIST3H2A interference on the EMT-related gene by western blot. Scale bars 100 μm

prostate cancer. Immunohistochemical analysis revealed that the expression of HIST3H2A and PCNA in LV-HIST3H2A tumor tissues was significantly lower than that in the control group (Fig. 5B and C). Additionally, the levels of p-RIP3 and p-MLKL were higher in the LV-HIST3H2A tumor tissue group compared to the control group, while the expression of Bax and Bcl-2 did not show significant differences (Fig. 5C). These findings suggest that HIST3H2A exerts its carcinogenic effect in vivo by inhibiting necroptosis rather than apoptosis.

Discussion

In many parts of the world, prostate cancer is a leading cancer among men. It is the second most commonly diagnosed solid organ cancer in men, following lung cancer [42–44]. Currently, approximately 10 million men worldwide are affected by this disease, with around 700,000 having metastatic disease [45–47]. While prostate cancer is typically diagnosed at an early stage, the search for potential molecular targets for treatment is crucial due to the long history of the disease and the uncertain clinical progression of individual patients. Therefore, we conducted a screening of differentially expressed genes in prostate cancer using the GEO database to identify new molecular targets. Through this screening, the HIST3H2A gene was successfully identified, showing significantly higher expression in prostate cancer tissues and cells compared to adjacent tissues and normal prostate cells.

The nucleosome, which is the fundamental unit of chromatin, consists of approximately 146 base pairs (bp) of DNA wrapped around a single copy of each of the histone proteins H3, H4, H2A, and H2B [48–50]. Histone variations can confer different structural properties on nucleosomes by either wrapping more or less DNA or altering their stability. These histone variations perform specific functions in DNA repair, chromosome separation, transcription initiation regulation, and tissue-specific roles [51–53]. Abnormal expression of H2A family proteins has been found to cause various types of cancer in humans, such as breast, colorectal, lung, testicular, bladder, ovarian, and prostate cancers [54–56]. The

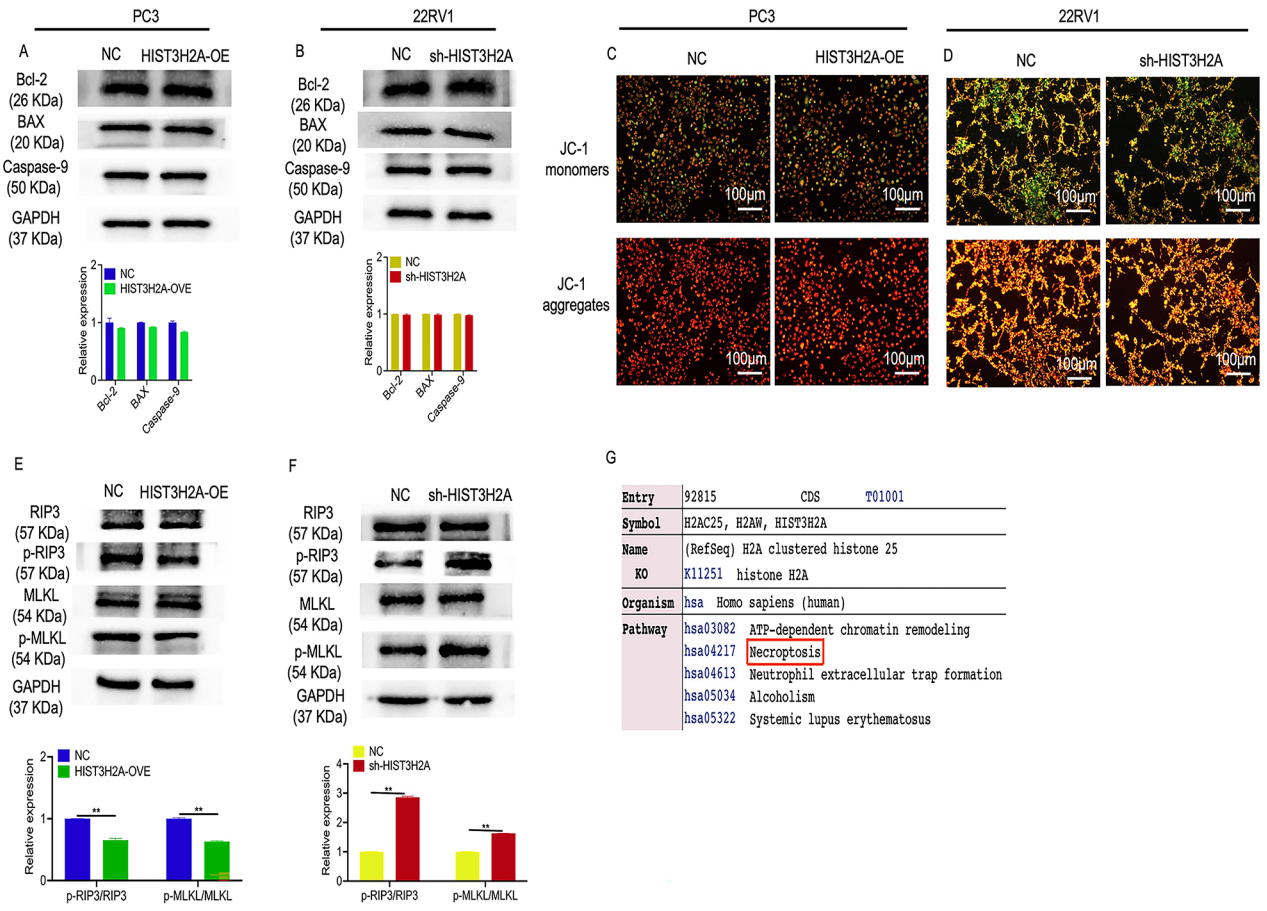

Fig. 4 HIST3H2A regulates cells proliferation through necroptosis but not through apoptosis. **A** The effect of HIST3H2A overexpression on the apoptosis-related gene by western blot. **B** The effect of HIST3H2A interference on the apoptosis-related gene by western blot. **C** The effect of HIST3H2A overexpression on the apoptosis by JC-1 assay. **D** The effect of HIST3H2A interference on the apoptosis by JC-1 assay. **E** The effect of HIST3H2A overexpression on the necroptosis-related gene by western blot. **F** The effect of HIST3H2A interference on the necroptosis-related gene by western blot. **G** KEGG database showed that HIST3H2A was involved in necroptosis regulation. Scale bars 100 μm

HIST3H2A protein, a member of the H2A family, has been identified as a potential biomarker for pancreatic cancer, non-small cell lung cancer, glioblastoma, breast cancer, and lung cancer. However, its role in prostate cancer remains unknown. Our research findings demonstrate that HIST3H2A plays a pro-cancer role in the development and progression of prostate cancer. Overexpression of HIST3H2A can enhance cell proliferation, migration, invasion, and promote the epithelial-mesenchymal transition (EMT) process in tumors. Conversely, interfering with HIST3H2A expression leads to the opposite effect.

necroptosis is a regulated form of cell death that differs from apoptosis as it does not depend on caspase [57, 58]. necroptosis requires RIPK3, which activates RIPK3 and leads to an increase in phosphorylated MLKL [59]. This phosphorylated MLKL then oligomerizes to form activated 'bad dead' complexes and translocates to the plasma membrane [60, 61]. This process ultimately results in cell death, characterized by plasma membrane penetration, cell swelling, and loss of cell and organelle integrity [62–64]. The significance of necroptosis in cancer is increasingly recognized, and a better understanding of this process may contribute to the development of new cancer control strategies. To further investigate the role of HIST3H2A in regulating the progression of prostate cancer, we conducted correlation analysis using the KEGG database. The results revealed that HIST3H2A is involved in regulating the necroptosis signaling pathway. Additionally, western blot and JC-1 tests demonstrated that HIST3H2A regulates the biology and function of prostate cancer cells through necroptosis rather than apoptosis.

To further confirm the role of HIST3H2A in vivo, we conducted xenograft tumor experiments in nude mice. The findings revealed that interfering with HIST3H2A significantly inhibited tumor growth in these mice. Additionally, IHC tests demonstrated that HIST3H2A inhibits the proliferation of prostate cancer cells in vivo by promoting necroptosis instead of apoptosis. In conclusion,

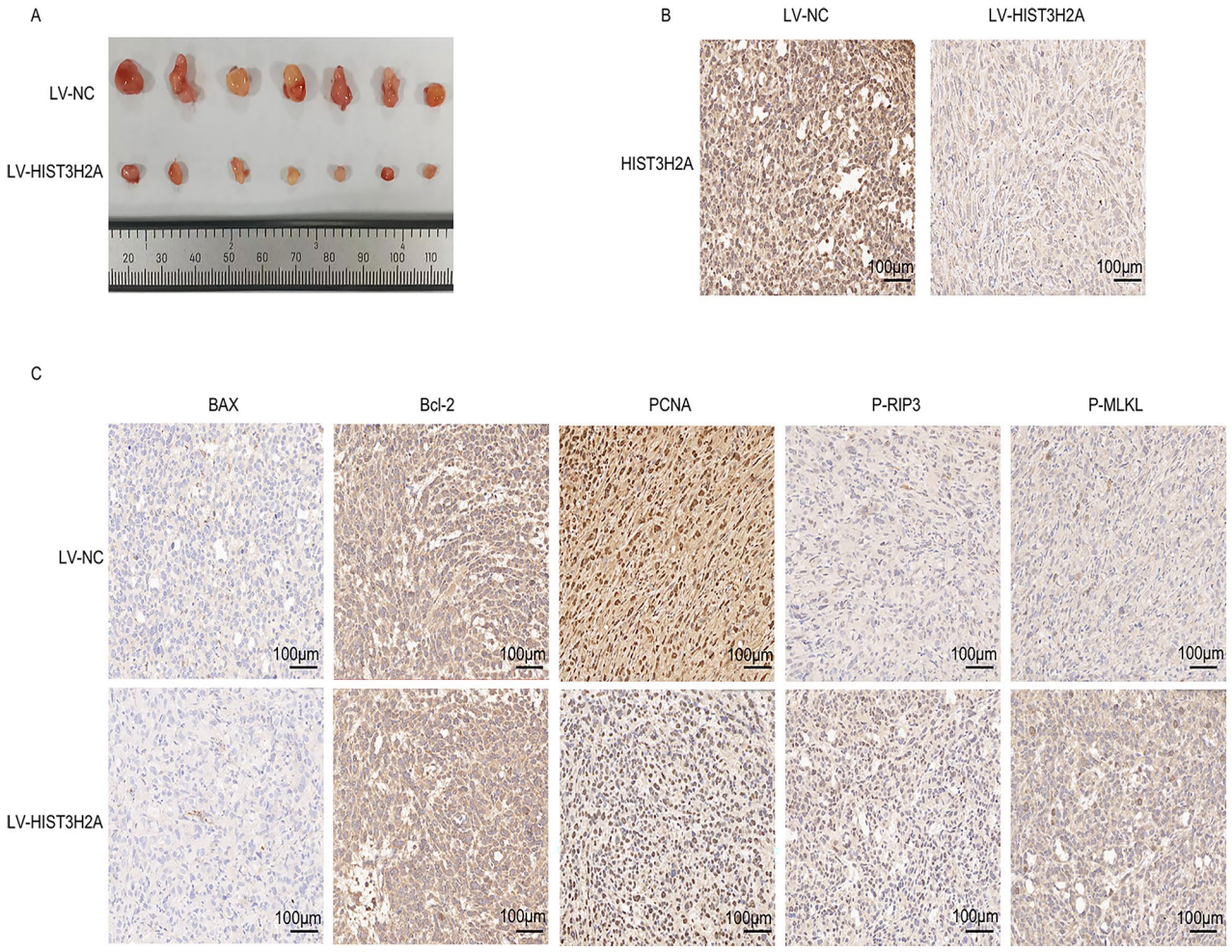

Fig. 5 HIST3H2A regulates cells proliferation through necroptosis but not through apoptosis in vivo. **A** Images of a given set of tumors ($n=7$). **B** IHC staining of HIST3H2A. **C** IHC staining of Bax, Bcl-2,PCNA, p-RIP3 and p-MLKL in the indicated treated tumors. Scare bars, 100 μm

our results suggest that HIST3H2A promotes the progression of prostate cancer by inhibiting cell necroptosis rather than apoptosis. Our study provides new potential molecular targets for the treatment of prostate cancer.

Supplementary Information

The online version contains supplementary material available at https://doi.org/10.1186/s12885-024-12308-4.

Supplementary Material 1

Supplementary Material 2

Supplementary Material 3

Acknowledgements
Not applicable.

Author contributions
HX: Responsible for designing the experiments. LY: Conducted the experiments and wrote the paper. YR, HX: Contributed revision of the article. All authors have read and approved the final manuscript.

Funding
This work was supported by the National Natural Science Foundation of China (grants 31860242).

Data availability
The datasets used and/or analysed during the current study available from the corresponding author on reasonable request.

Declarations

Ethics approval and consent to participate
The Committee for Animal Care and Use of Guizhou University approved the animal study protocol (EAE-Gzu-2022-E022). we confirming the study is reported in accordance with ARRIVE guidelines.

Consent for publication
Not applicable.

Competing interests
The authors declare no competing interests.

Received: 24 October 2023 / Accepted: 24 April 2024
Published online: 29 April 2024

References

1. Chang AJ, Autio KA, Roach M 3rd, Scher HI. High-risk prostate cancer-classification and therapy. Nat Rev Clin Oncol. 2014;11(6):308–23. https://doi.org/10.1038/nrclinonc.2014.68.
2. Schatten H. Brief overview of prostate Cancer statistics, Grading, diagnosis and treatment strategies. Adv Exp Med Biol. 2018;1095:1–14. https://doi.org/10.1007/978-3-319-95693-0_1.
3. Vietri MT, D'Elia G, Caliendo G, Resse M, Casamassimi A, Passariello L, Albanese L, Cioffi M, Molinari AM. Hereditary prostate Cancer: genes related, Target Therapy and Prevention. Int J Mol Sci. 2021;22(7):3753. https://doi.org/10.3390/ijms22073753.
4. D'Arcy MS. Cell death: a review of the major forms of apoptosis, necrosis and autophagy. Cell Biol Int. 2019;43(6):582–92. https://doi.org/10.1002/cbin.11137.
5. Tong X, Tang R, Xiao M, Xu J, Wang W, Zhang B, Liu J, Yu X, Shi S. Targeting cell death pathways for cancer therapy: recent developments in necroptosis, pyroptosis, ferroptosis, and cuproptosis research. J Hematol Oncol. 2022;15(1):174. https://doi.org/10.1186/s13045-022-01392-3.
6. Li M, Wang ZW, Fang LJ, Cheng SQ, Wang X, Liu NF. Programmed cell death in atherosclerosis and vascular calcification. Cell Death Dis. 2022;13(5):467. https://doi.org/10.1038/s41419-022-04923-5.
7. Green DR, The Coming Decade of Cell Death Research. Five Riddles Cell. 2019;177(5):1094–107. https://doi.org/10.1016/j.cell.2019.04.024.
8. Hahn M, Dambacher S, Schotta G. Heterochromatin dysregulation in human diseases. J Appl Physiol (1985). 2010;109(1):232–42. https://doi.org/10.1152/japplphysiol.00053.2010.
9. Edwards DR, Handsley MM, Pennington CJ. The ADAM metalloproteinases. Mol Aspects Med. 2008;29(5):258–89. https://doi.org/10.1016/j.mam.2008.08.001.
10. Rosenfeld E, Ganguly A, De Leon DD. Congenital hyperinsulinism disorders: genetic and clinical characteristics. Am J Med Genet C Semin Med Genet. 2019;181(4):682–92. https://doi.org/10.1002/ajmg.c.31737.
11. Schuschel K, Helwig M, Hüttelmaier S, Heckl D, Klusmann JH, Hoell JI. RNA-Binding proteins in Acute Leukemias. Int J Mol Sci. 2020;21(10):3409. https://doi.org/10.3390/ijms21103409.
12. Liu Y, Liu T, Lei T, Zhang D, Du S, Girani L, Qi D, Lin C, Tong R, Wang Y. RIP1/RIP3-regulated necroptosis as a target for multifaceted disease therapy (review). Int J Mol Med. 2019;44(3):771–86. https://doi.org/10.3892/ijmm.2019.4244.
13. Guo C, Fu R, Zhou M, Wang S, Huang Y, Hu H, Zhao J, Gaskin F, Yang N, Fu SM. Pathogenesis of lupus nephritis: RIP3 dependent necroptosis and NLRP3 inflammasome activation. J Autoimmun. 2019;103:102286. https://doi.org/10.1016/j.jaut.2019.05.014.
14. Chen D, Gregory AD, Li X, Wei J, Burton CL, Gibson G, Scott SJ, St Croix CM, Zhang Y, Shapiro SD. RIP3-dependent necroptosis contributes to the pathogenesis of chronic obstructive pulmonary disease. JCI Insight. 2021;6(12):e144689. https://doi.org/10.1172/jci.insight.144689.
15. Sun L, Wang H, Wang Z, He S, Chen S, Liao D, Wang L, Yan J, Liu W, Lei X, Wang X. Mixed lineage kinase domain-like protein mediates necrosis signaling downstream of RIP3 kinase. Cell. 2012;148(1–2):213–27. https://doi.org/10.1016/j.cell.2011.11.031.
16. Gong Y, Fan Z, Luo G, Yang C, Huang Q, Fan K, Cheng H, Jin K, Ni Q, Yu X, Liu C. The role of necroptosis in cancer biology and therapy. Mol Cancer. 2019;18(1):100. https://doi.org/10.1186/s12943-019-1029-8.
17. Liu S, Joshi K, Denning MF, Zhang J. RIPK3 signaling and its role in the pathogenesis of cancers. Cell Mol Life Sci. 2021;78(23):7199–217. https://doi.org/10.1007/s00018-021-03947-y.
18. Wang Y, Zhao M, He S, Luo Y, Zhao Y, Cheng J, Gong Y, Xie J, Wang Y, Hu B, Tian L, Liu X, Li C, Huang Q. Necroptosis regulates tumor repopulation after radiotherapy via RIP1/RIP3/MLKL/JNK/IL8 pathway. J Exp Clin Cancer Res. 2019;38(1):461. https://doi.org/10.1186/s13046-019-1423-5.
19. Liu C, Chen Y, Cui W, Cao Y, Zhao L, Wang H, Liu X, Fan S, Huang K, Tong A, Zhou L. Inhibition of neuronal necroptosis mediated by RIP1/RIP3/MLKL provides neuroprotective effects on kaolin-induced hydrocephalus in mice. Cell Prolif. 2021;54(9):e13108. https://doi.org/10.1111/cpr.13108.
20. Xue H, Shi H, Zhang F, Li H, Li C, Han Q. RIP3 contributes to Cardiac Hypertrophy by influencing MLKL-Mediated calcium influx. Oxid Med Cell Longev. 2022;2022:5490553. https://doi.org/10.1155/2022/5490553.
21. Cutter AR, Hayes JJ. A brief review of nucleosome structure. FEBS Lett. 2015;589(20 Pt A):2914-22. https://doi.org/10.1016/j.febslet.2015.05.016.
22. Kale S, Goncearenco A, Markov Y, Landsman D, Panchenko AR. Molecular recognition of nucleosomes by binding partners. Curr Opin Struct Biol. 2019;56:164–70. https://doi.org/10.1016/j.sbi.2019.03.010.
23. Tessarz P, Kouzarides T. Histone core modifications regulating nucleosome structure and dynamics. Nat Rev Mol Cell Biol. 2014;15(11):703–8. https://doi.org/10.1038/nrm3890.
24. Wang X, Bai L, Bryant GO, Ptashne M. Nucleosomes and the accessibility problem. Trends Genet. 2011;27(12):487–92. https://doi.org/10.1016/j.tig.2011.09.001.
25. Feng Y, Endo M, Sugiyama H. Nucleosomes and epigenetics from a Chemical Perspective. ChemBioChem. 2021;22(4):595–612. https://doi.org/10.1002/cbic.202000332.
26. Huertas J, Cojocaru V. Breaths, twists, and turns of atomistic nucleosomes. J Mol Biol. 2021;433(6):166744. https://doi.org/10.1016/j.jmb.2020.166744.
27. Fedyuk V, Erez N, Furth N, Beresh O, Andreishcheva E, Shinde A, Jones D, Zakai BB, Mavor Y, Peretz T, Hubert A, Cohen JE, Salah A, Temper M, Grinshpun A, Maoz M, Zick A, Ron G, Shema E. Multiplexed, single-molecule, epigenetic analysis of plasma-isolated nucleosomes for cancer diagnostics. Nat Biotechnol. 2023;41(2):212–21. https://doi.org/10.1038/s41587-022-01447-3.
28. He S, Wu Z, Tian Y, Yu Z, Yu J, Wang X, Li J, Liu B, Xu Y. Structure of nucleosome-bound human BAF complex. Science. 2020;367(6480):875–81. https://doi.org/10.1126/science.aaz9761.
29. Giaimo BD, Ferrante F, Herchenröther A, Hake SB, Borggrefe T. The histone variant H2A.Z in gene regulation. Epigenetics Chromatin. 2019;12(1):37. https://doi.org/10.1186/s13072-019-0274-9.
30. Dryhurst D, Ausió J. Histone H2A.Z deregulation in prostate cancer. Cause or effect? Cancer Metastasis Rev. 2014;33(2–3):429–39. https://doi.org/10.1007/s10555-013-9486-9.
31. Rangasamy D. Histone variant H2A.Z can serve as a new target for breast cancer therapy. Curr Med Chem. 2010;17(28):3155–61. https://doi.org/10.2174/092986710792231941.
32. Ogitani Y, Aida T, Hagihara K, Yamaguchi J, Ishii C, Harada N, Soma M, Okamoto H, Oitate M, Arakawa S, Hirai T, Atsumi R, Nakada T, Hayakawa I, Abe Y, Agatsuma T. DS-8201a, A Novel HER2-Targeting ADC with a novel DNA topoisomerase I inhibitor, demonstrates a Promising Antitumor Efficacy with differentiation from T-DM1. Clin Cancer Res. 2016;22(20):5097–108. https://doi.org/10.1158/1078-0432.CCR-15-2822.
33. Ge Y, Liu BL, Cui JP, Li SQ. Livin promotes colon cancer progression by regulation of H2A.XY39ph via JMJD6. Life Sci. 2019;234:116788. https://doi.org/10.1016/j.lfs.2019.116788.
34. Guo ZF, Kong FL. Akt regulates RSK2 to alter phosphorylation level of H2A.X in breast cancer. Oncol Lett. 2021;21(3):187. https://doi.org/10.3892/ol.2021.12448.
35. Gao X, Bao H, Liu L, Zhu W, Zhang L, Yue L. Systematic analysis of lysine acetylome and succinylome reveals the correlation between modification of H2A.X complexes and DNA damage response in breast cancer. Oncol Rep. 2020;43(6):1819–30. https://doi.org/10.3892/or.2020.7554. Epub 2020 Mar 19.
36. Liu Y, Long YH, Wang SQ, Zhang YY, Li YF, Mi JS, Yu CH, Li DY, Zhang JH, Zhang XJ. JMJD6 regulates histone H2A.X phosphorylation and promotes autophagy in triple-negative breast cancer cells via a novel tyrosine kinase activity. Oncogene. 2019;38(7):980–97. https://doi.org/10.1038/s41388-018-0466-y.
37. Miyake K, Takano N, Kazama H, Kikuchi H, Hiramoto M, Tsukahara K, Miyazawa K. Ricolinostat enhances adavosertib–induced mitotic catastrophe in TP53–mutated head and neck squamous cell carcinoma cells. Int J Oncol. 2022;60(5):54. https://doi.org/10.3892/ijo.2022.5344.
38. Weinreb O, Amit T, Bar-Am O, Sagi Y, Mandel S, Youdim MB. Involvement of multiple survival signal transduction pathways in the neuroprotective, neurorescue and APP processing activity of rasagiline and its propargyl moiety. J Neural Transm Suppl. 2006;70457–65. https://doi.org/10.1007/978-3-211-45295-0_69.
39. Kim JH, Jeon S, Choi HD, Lee JH, Bae JS, Kim N, Kim HG, Kim KB, Kim HR. Exposure to long-term evolution radiofrequency electromagnetic fields decreases neuroblastoma cell proliferation via Akt/mTOR-mediated cellular senescence. J Toxicol Environ Health A. 2021;84(20):846–57. https://doi.org/10.1080/15287394.2021.1944944.
40. Schmittgen TD, Livak KJ. Analyzing real-time PCR data by the comparative C(T) method. Nat Protoc. 2008;3(6):1101–8. https://doi.org/10.1038/nprot.2008.73.
41. Sailer V, von Amsberg G, Duensing S, Kirfel J, Lieb V, Metzger E, Offermann A, Pantel K, Schuele R, Taubert H, Wach S, Perner S, Werner S, Aigner A. Experimental in vitro, ex vivo and in vivo models in prostate cancer research. Nat Rev Urol. 2023;20(3):158–78. https://doi.org/10.1038/s41585-022-00677-z.

42. Nguyen-Nielsen M, Borre M. Diagnostic and therapeutic strategies for prostate Cancer. Semin Nucl Med. 2016;46(6):484–90. https://doi.org/10.1053/j.semnuclmed.2016.07.002.
43. Prostate cancer. Nat Rev Dis Primers. 2021;7(1):8. https://doi.org/10.1038/s41572-021-00249-2.
44. Kaiser A, Haskins C, Siddiqui MM, Hussain A, D'Adamo C. The evolving role of diet in prostate cancer risk and progression. Curr Opin Oncol. 2019;31(3):222–9. https://doi.org/10.1097/CCO.0000000000000519.
45. Smith ZL, Eggener SE, Murphy AB. African-American prostate Cancer disparities. Curr Urol Rep. 2017;18(10):81. https://doi.org/10.1007/s11934-017-0724-5.
46. Ghafouri-Fard S, Shabestari FA, Vaezi S, Abak A, Shoorei H, Karimi A, Taheri M, Basiri A. Emerging impact of quercetin in the treatment of prostate cancer. Biomed Pharmacother. 2021;138:111548. https://doi.org/10.1016/j.biopha.2021.111548.
47. Wilt TJ, Ullman KE, Linskens EJ, MacDonald R, Brasure M, Ester E, Nelson VA, Saha J, Sultan S, Dahm P. Therapies for clinically localized prostate Cancer: a comparative effectiveness review. J Urol. 2021;205(4):967–76. https://doi.org/10.1097/JU.0000000000001578.
48. Jansen A, Verstrepen KJ. Nucleosome positioning in Saccharomyces cerevisiae. Microbiol Mol Biol Rev. 2011;75(2):301–20. https://doi.org/10.1128/MMBR.00046-10.
49. Andrews AJ, Luger K. Nucleosome structure(s) and stability: variations on a theme. Annu Rev Biophys. 2011;40:99–117. https://doi.org/10.1146/annurev-biophys-042910-155329.
50. Korber P. Active nucleosome positioning beyond intrinsic biophysics is revealed by in vitro reconstitution. Biochem Soc Trans. 2012;40(2):377–82. https://doi.org/10.1042/BST20110730.
51. Szerlong HJ, Hansen JC. Nucleosome distribution and linker DNA: connecting nuclear function to dynamic chromatin structure. Biochem Cell Biol. 2011;89(1):24–34. https://doi.org/10.1139/O10-139.
52. Wolffe AP, Kurumizaka H. The nucleosome: a powerful regulator of transcription. Prog Nucleic Acid Res Mol Biol. 1998;61:379–422. https://doi.org/10.1016/s0079-6603(08)60832-6.
53. Schwab DJ, Bruinsma RF, Rudnick J, Widom J. Nucleosome switches. Phys Rev Lett. 2008;100(22):228105. https://doi.org/10.1103/PhysRevLett.100.228105.
54. Jiang X, Wen J, Paver E, Wu YH, Sun G, Bullman A, Dahlstrom JE, Tremethick DJ, Soboleva TA. H2A.B is a cancer/testis factor involved in the activation of ribosome biogenesis in Hodgkin lymphoma. EMBO Rep. 2021;22(8):e52462. https://doi.org/10.15252/embr.202152462.
55. Han S, Cao C, Liu R, Yuan Y, Pan L, Xu M, Hu C, Zhang X, Li M, Zhang X. GAS41 mediates proliferation and GEM chemoresistance via H2A.Z.2 and Notch1 in pancreatic cancer. Cell Oncol (Dordr). 2022;45(3):429–46. https://doi.org/10.1007/s13402-022-00675-8.
56. Berta DG, Kuisma H, Välimäki N, Räisänen M, Jäntti M, Pasanen A, Karhu A, Kaukomaa J, Taira A, Cajuso T, Nieminen S, Penttinen RM, Ahonen S, Lehtonen R, Mehine M, Vahteristo P, Jalkanen J, Sahu B, Ravantti J, Mäkinen N, Rajamäki K, Palin K, Taipale J, Heikinheimo O, Bützow R, Kaasinen E, Aaltonen LA. Deficient H2A.Z deposition is associated with genesis of uterine leiomyoma. Nature. 2021;596(7872):398–403. https://doi.org/10.1038/s41586-021-03747-1.
57. Hu X, Wang Z, Kong C, Wang Y, Zhu W, Wang W, Li Y, Wang W, Lu S. Necroptosis: a new target for prevention of osteoporosis. Front Endocrinol (Lausanne). 2022;13:1032614. https://doi.org/10.3389/fendo.2022.1032614.
58. Seo J, Nam YW, Kim S, Oh DB, Song J. Necroptosis molecular mechanisms: recent findings regarding novel necroptosis regulators. Exp Mol Med. 2021;53(6):1007–17. https://doi.org/10.1038/s12276-021-00634-7.
59. Sarcognato S, Jong IEM, Fabris L, Cadamuro M, Guido M. Necroptosis Cholangiocarcinoma Cells. 2020;9(4):982. https://doi.org/10.3390/cells9040982.
60. Martens S, Bridelance J, Roelandt R, Vandenabeele P, Takahashi N. MLKL in cancer: more than a necroptosis regulator. Cell Death Differ. 2021;28(6):1757–72. https://doi.org/10.1038/s41418-021-00785-0.
61. Lee SA, Chang LC, Jung W, Bowman JW, Kim D, Chen W, Foo SS, Choi YJ, Choi UY, Bowling A, Yoo JS, Jung JU. OASL phase condensation induces amyloid-like fibrillation of RIPK3 to promote virus-induced necroptosis. Nat Cell Biol. 2023;25(1):92–107. https://doi.org/10.1038/s41556-022-01039-y.
62. Verdonck S, Nemegeer J, Vandenabeele P, Maelfait J. Viral manipulation of host cell necroptosis and pyroptosis. Trends Microbiol. 2022;30(6):593–605. https://doi.org/10.1016/j.tim.2021.11.011.
63. Anosike NL, Adejuwon JF, Emmanuel GE, Adebayo OS, Etti-Balogun H, Nathaniel JN, Omotosho OI, Aschner M, Ijomone OM. Necroptosis in the developing brain: role in neurodevelopmental disorders. Metab Brain Dis. 2023;38(3):831–7. https://doi.org/10.1007/s11011-023-01203-9.
64. Negroni A, Colantoni E, Cucchiara S, Stronati L. Necroptosis in intestinal inflammation and Cancer: New concepts and therapeutic perspectives. Biomolecules. 2020;10(10):1431. https://doi.org/10.3390/biom10101431.

Publisher's Note